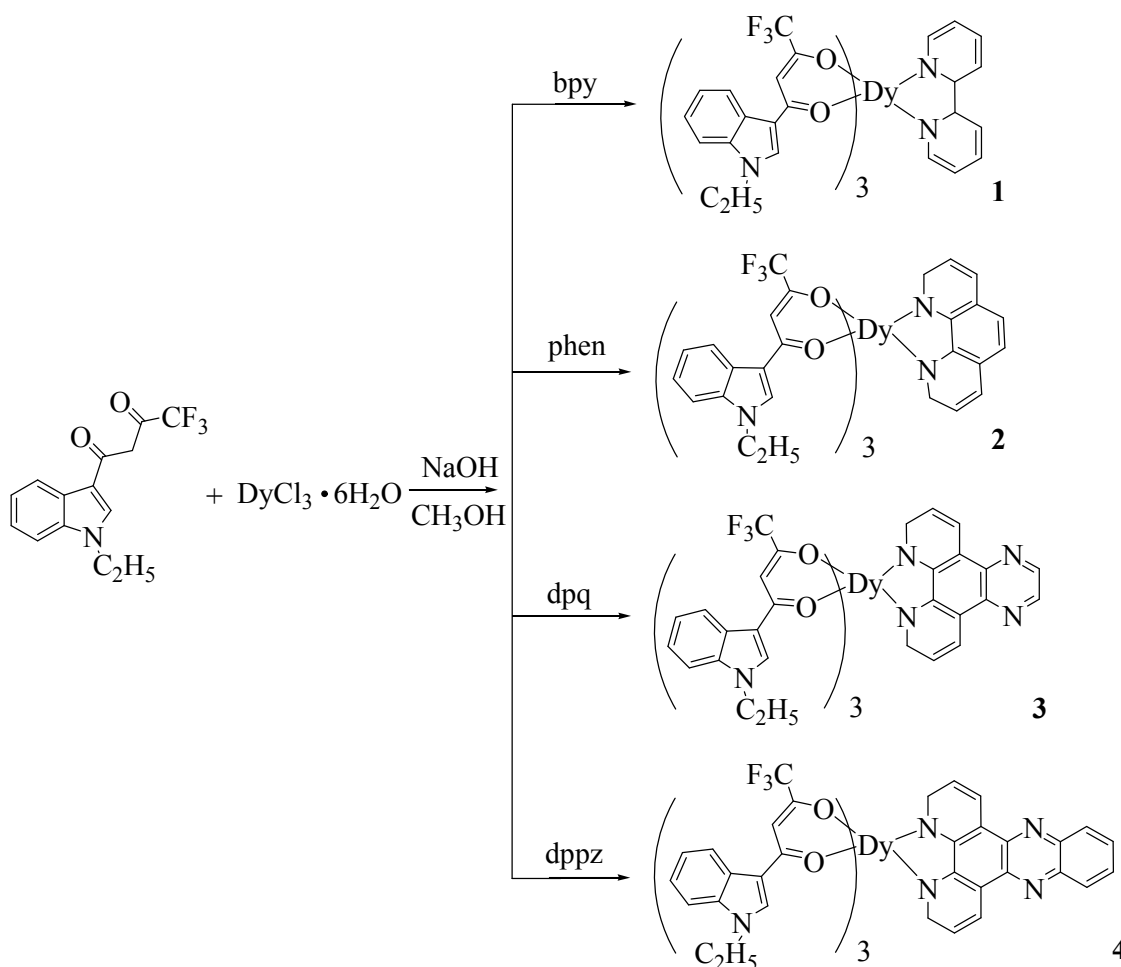


## Electronic Supplementary Information

### Auxiliary Ligands Field Dominated Single-Molecule Magnets of a Series of Indole-Derivative $\beta$ -diketone Mononuclear Dy(III) Complexes

Yanping Dong,<sup>a,b</sup> Pengfei Yan,<sup>a</sup> Xiaoyan Zou,<sup>a</sup> Guangfeng Hou,<sup>a</sup> Guangming Li<sup>\*a</sup>

<sup>a</sup> Key Laboratory of Functional Inorganic Material Chemistry (MOE), School of Chemistry and Materials Science, Heilongjiang University, No. 74, Xuefu Road, Nangang District, Harbin, Heilongjiang 150080, P. R. China, E-mail: [gml\\_i\\_2000@163.com](mailto:gml_i_2000@163.com). Fax: (+86)451-86608458; Tel: (+86)451-86608458; <sup>b</sup> Department of Food and Pharmaceutical Engineering, Suihua University, Suihua, Heilongjiang 152061, P. R. China



**Scheme S1.** Synthesis of complexes 1-4

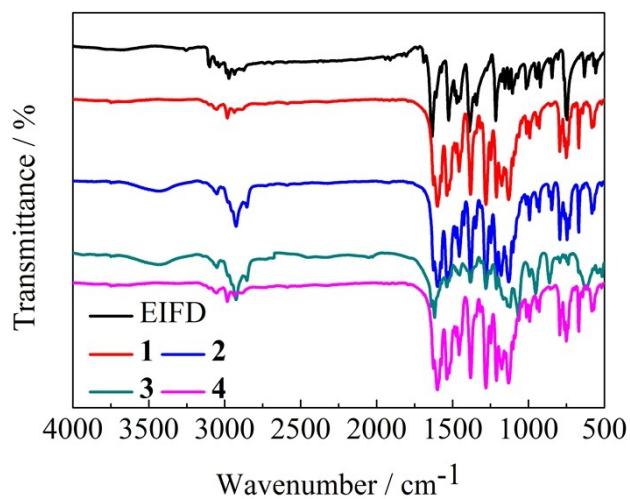


**Figure S1.** IR spectra of EIFD and complexes 1–4

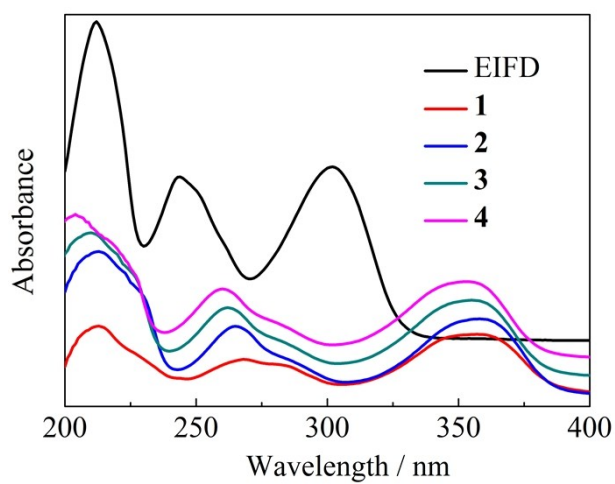


**Figure S2.** UV absorption spectra of EIFD and complexes 1–4

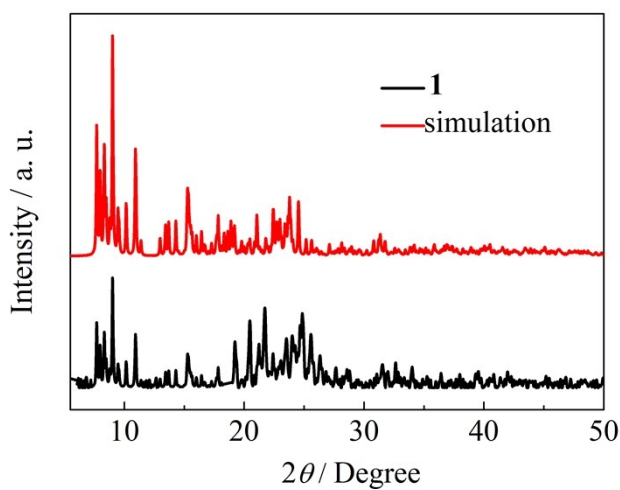


**Figure S3.** The powder X-ray diffraction patterns and the simulated patterns of complex 1

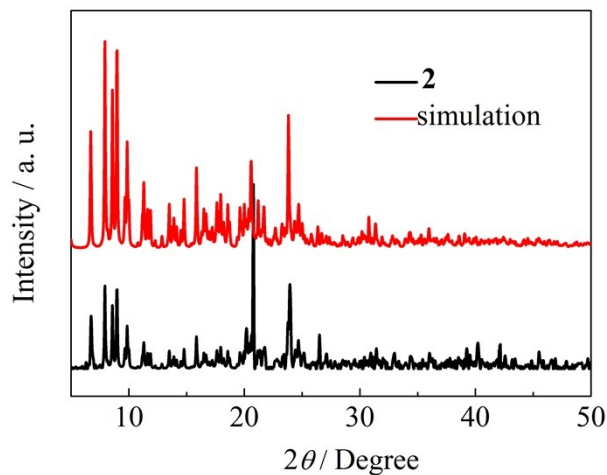


**Figure S4.** The powder X-ray diffraction patterns and the simulated patterns of complex 2

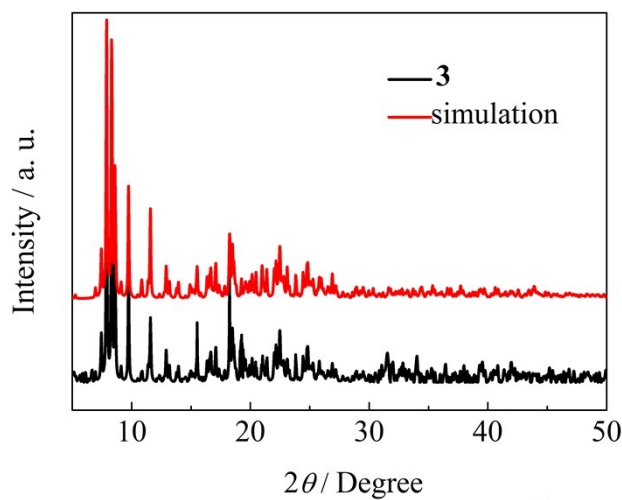


**Figure S5.** The powder X-ray diffraction patterns and the simulated patterns of complex 3

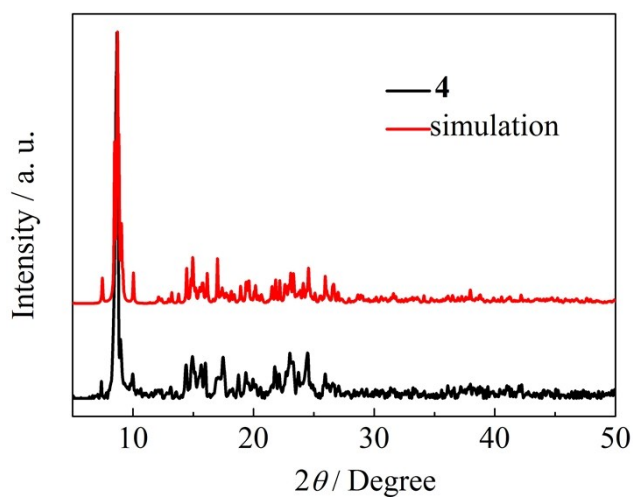


**Figure S6.** The powder X-ray diffraction patterns and the simulated patterns of complex 4

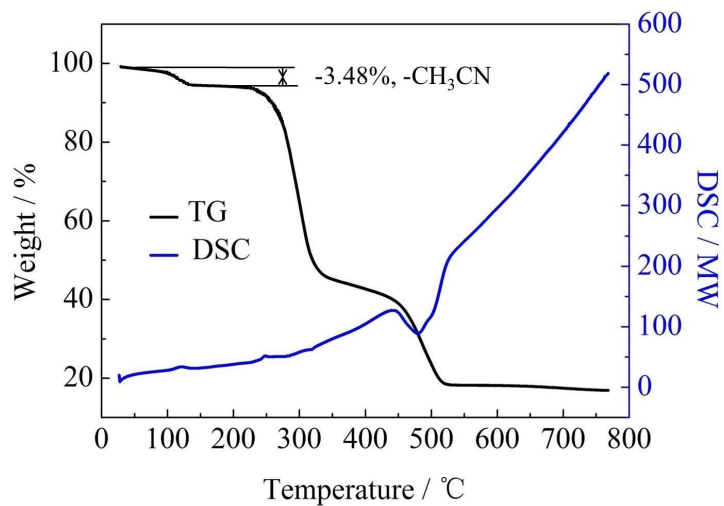


**Figure S7.** TG-DSC curves of complex 1

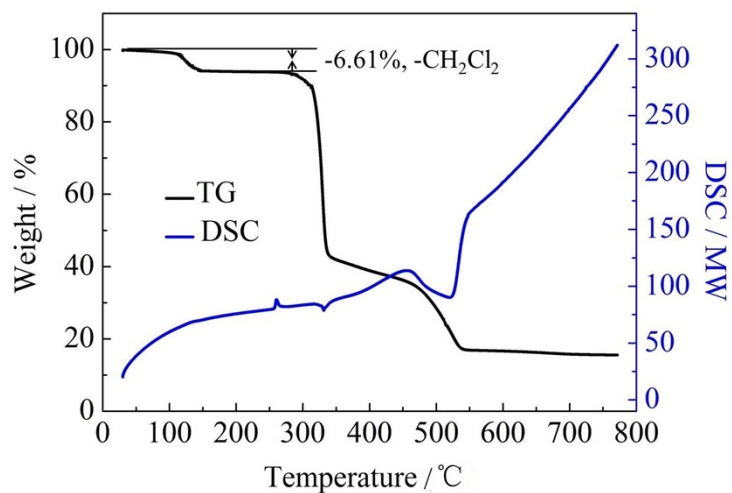


**Figure S8.** TG-DSC curves of complex 2

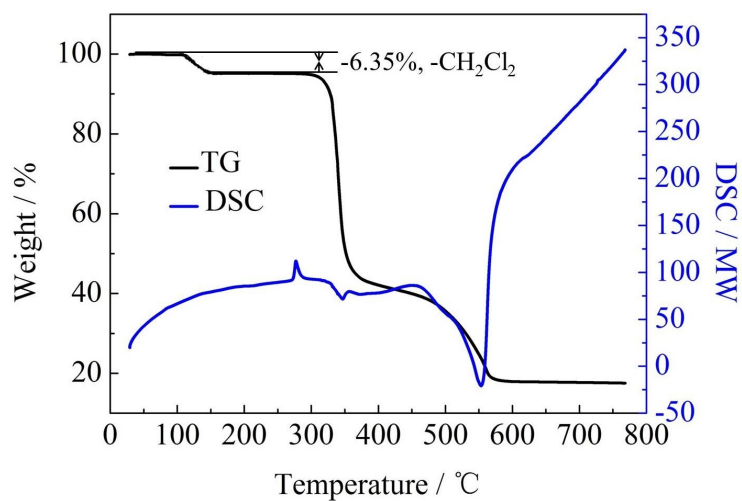


**Figure S9.** TG-DSC curves of complex 3

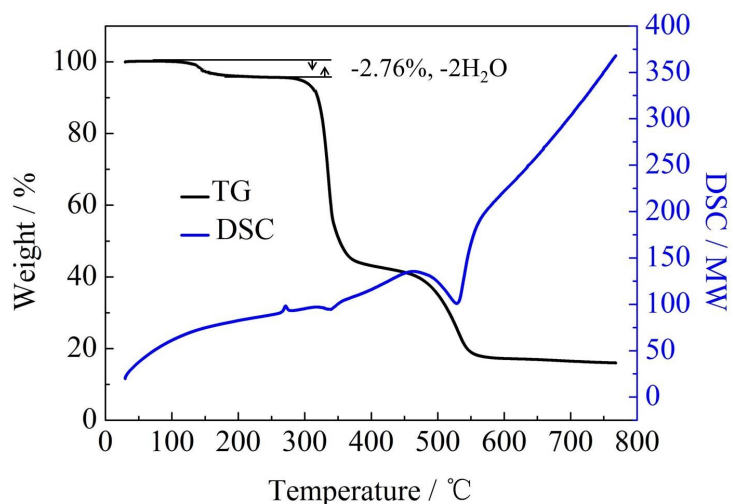


**Figure S10.** TG-DSC curves of complex **4**

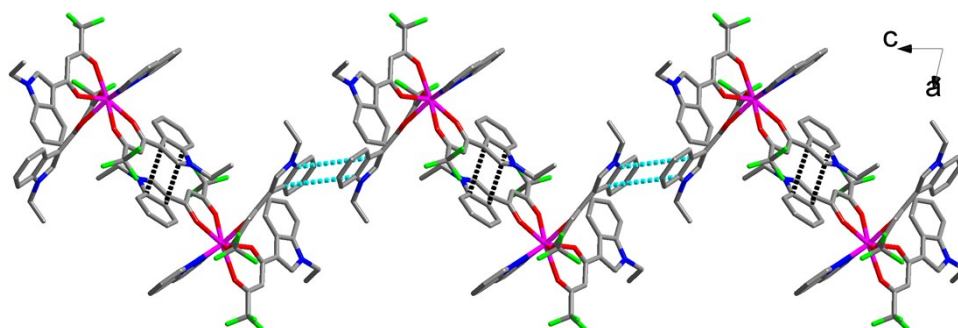


**Figure S11.** 1D supramolecular chain of complex **1** formed through the  $\pi$ - $\pi$  interactions between the indole rings

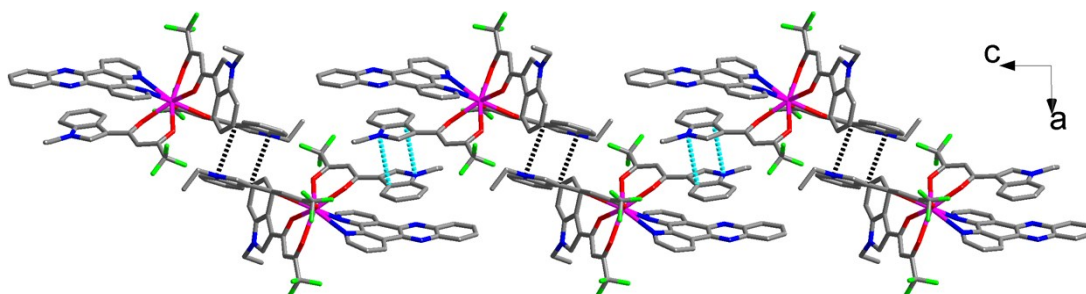


**Figure S12.** 1D supramolecular chain of complex **4** formed through the  $\pi$ - $\pi$  interactions between the indole rings

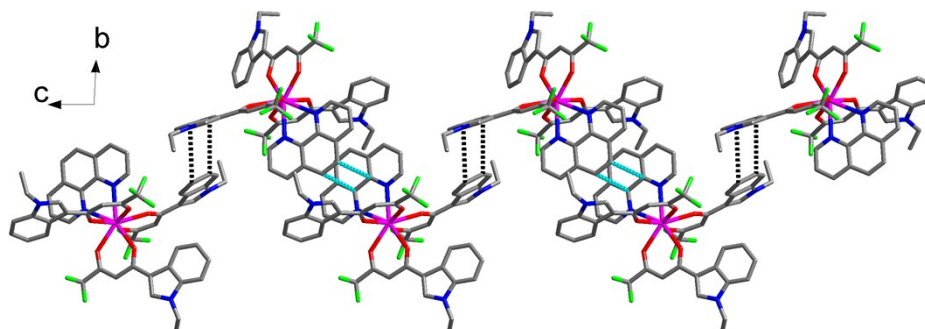


**Figure S13.** 1D supramolecular chain of complex **2** formed through the  $\pi$ - $\pi$  interactions between the indole rings as well as between the phen rings

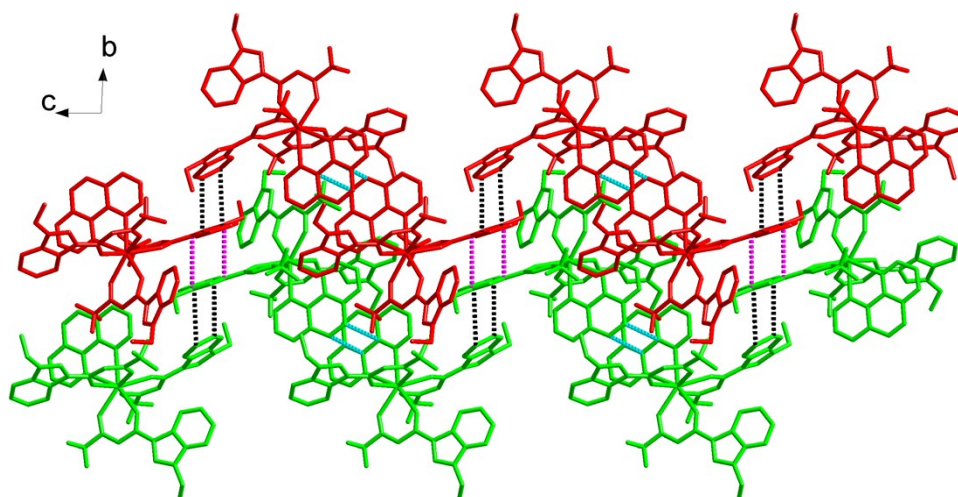


**Figure S14.** 2D supramolecular layer of complex **2** formed by the  $\pi$ - $\pi$  interactions between the indole rings

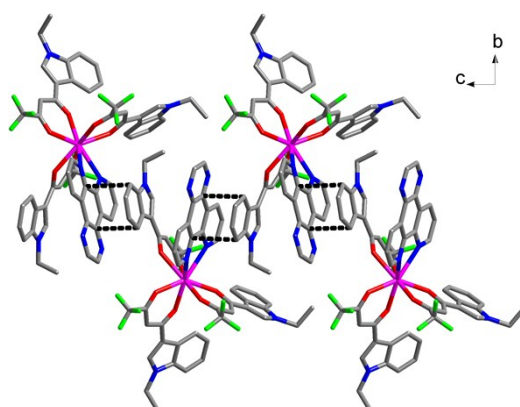


**Figure S15.** 1D supramolecular chain of complex **3** formed through the  $\pi$ - $\pi$  interactions between the indole and dpqn rings

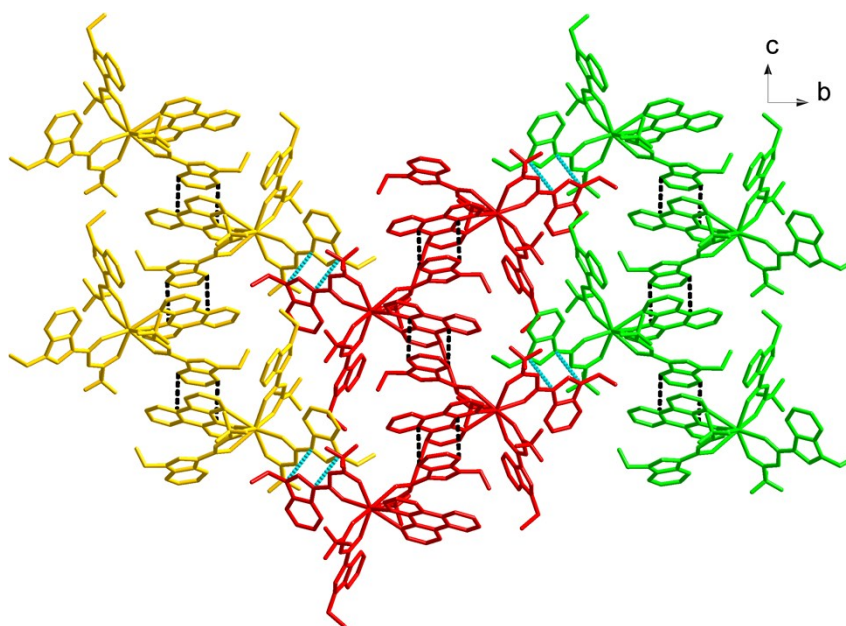


**Figure S16.** 2D supramolecular layer of complex **3** formed by the  $\pi$ - $\pi$  interactions between the indole rings

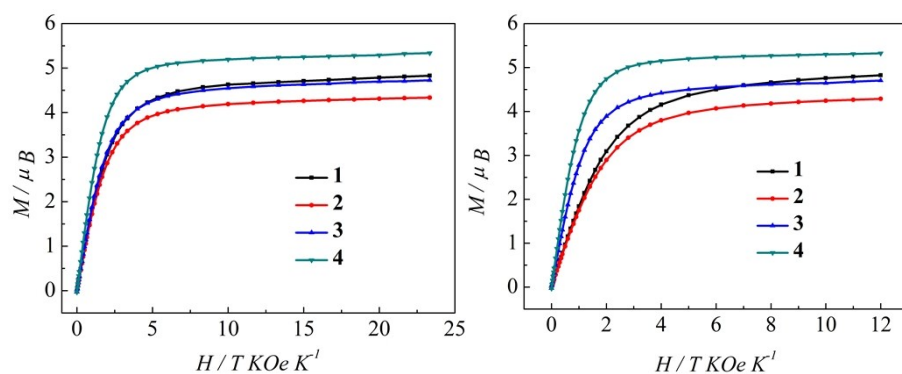


**Figure S17.**  $M$  vs  $H/T$  data for complexes **1–4** at 3 K (left) and 5 K (right)

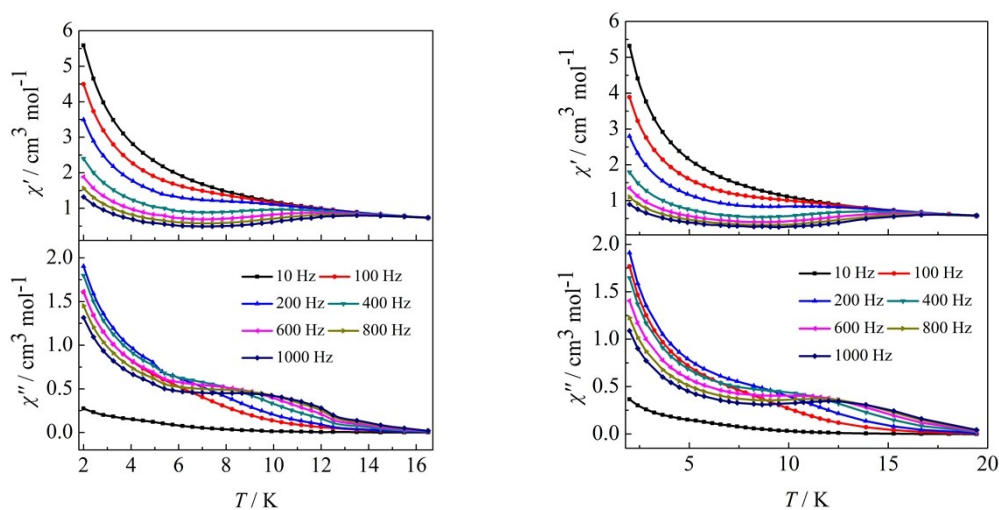


**Figure S18.** Temperature dependence of the in-phase ( $\chi'$ ) and out-of-phase ( $\chi''$ ) ac susceptibility of complexes **1** (left) and **2** (right) under 0 Oe in the frequency range 10–1000 Hz

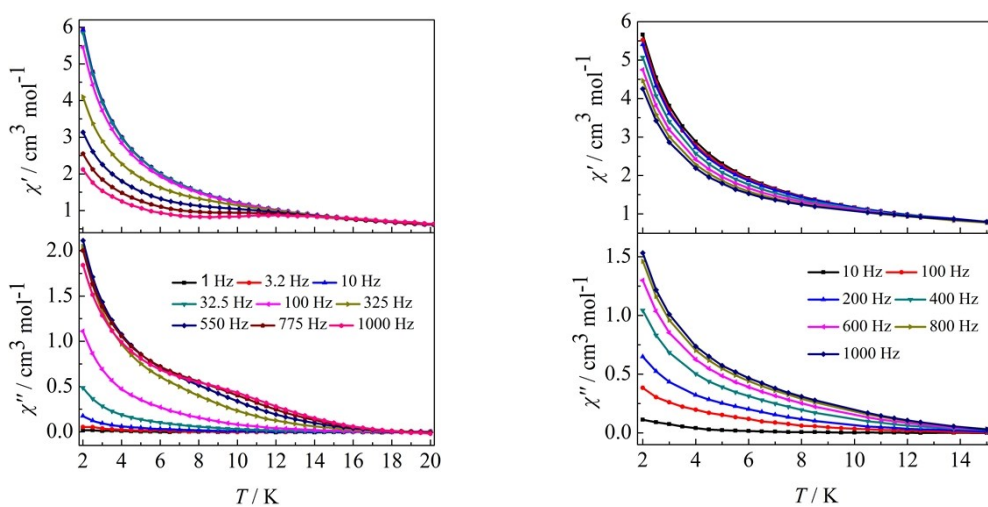


**Figure S19.** Temperature dependence of the in-phase ( $\chi'$ ) and out-of-phase ( $\chi''$ ) ac susceptibility of complex **3** under 0 Oe in the frequency range 1–1000 Hz (left) and complex **4** under 0 Oe in the frequency range 10–1000 Hz (right)

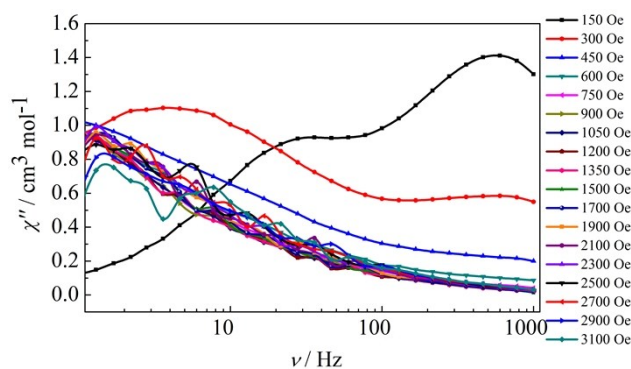


**Figure S20.** Frequency dependence of the out-of-phase ( $\chi''$ ) ac susceptibility at 2 K in the frequency range 1–1000 Hz and under different field between 150 and 3100 Oe for complex **3**

**Table S1.** Selected bond lengths and angles for complexes **1–4**

1		2		3		4	
Dy(1)-O(1)	2.329(6)	Dy(1)-O(1)	2.338(3)	Dy(1)-O(1)	2.302(4)	Dy(1)-O(1)	2.344(5)
Dy(1)-O(2)	2.322(5)	Dy(1)-O(2)	2.323(3)	Dy(1)-O(2)	2.306(3)	Dy(1)-O(2)	2.341(5)
Dy(1)-O(3)	2.323(6)	Dy(1)-O(3)	2.313(3)	Dy(1)-O(3)	2.287(3)	Dy(1)-O(3)	2.304(4)
Dy(1)-O(4)	2.327(6)	Dy(1)-O(4)	2.356(3)	Dy(1)-O(4)	2.305(4)	Dy(1)-O(4)	2.299(5)
Dy(1)-O(5)	2.338(7)	Dy(1)-O(5)	2.339(3)	Dy(1)-O(5)	2.342(3)	Dy(1)-O(5)	2.300(5)
Dy(1)-O(6)	2.324(6)	Dy(1)-O(6)	2.344(3)	Dy(1)-O(6)	2.346(3)	Dy(1)-O(6)	2.300(4)
Dy(1)-N(1)	2.580(7)	Dy(1)-N(4)	2.563(3)	Dy(1)-N(4)	2.559(4)	Dy(1)-N(1)	2.587(6)
Dy(1)-N(2)	2.566(7)	Dy(1)-N(5)	2.569(3)	Dy(1)-N(5)	2.589(4)	Dy(1)-N(2)	2.567(6)
O(2)-Dy(1)-O(3)	112.9(2)	O(3)-Dy(1)-O(2)	121.15(11)	O(3)-Dy(1)-O(1)	89.20(14)	O(4)-Dy(1)-O(6)	89.64(17)
O(2)-Dy(1)-O(6)	85.5(2)	O(3)-Dy(1)-O(1)	76.38(11)	O(3)-Dy(1)-O(4)	73.27(13)	O(4)-Dy(1)-O(5)	82.16(19)
O(3)-Dy(1)-O(6)	139.9(2)	O(2)-Dy(1)-O(1)	72.19(10)	O(1)-Dy(1)-O(4)	79.92(14)	O(6)-Dy(1)-O(5)	72.70(16)
O(2)-Dy(1)-O(4)	75.3(2)	O(3)-Dy(1)-O(5)	140.52(11)	O(3)-Dy(1)-O(2)	79.11(13)	O(4)-Dy(1)-O(3)	73.10(16)
O(3)-Dy(1)-O(4)	72.4(2)	O(2)-Dy(1)-O(5)	75.61(10)	O(1)-Dy(1)-O(2)	72.76(13)	O(6)-Dy(1)-O(3)	78.63(16)
O(6)-Dy(1)-O(4)	147.6(2)	O(1)-Dy(1)-O(5)	141.18(10)	O(4)-Dy(1)-O(2)	141.10(13)	O(5)-Dy(1)-O(3)	141.98(19)
O(2)-Dy(1)-O(1)	72.6(2)	O(3)-Dy(1)-O(6)	80.11(11)	O(3)-Dy(1)-O(5)	77.17(13)	O(4)-Dy(1)-O(2)	138.15(17)
O(3)-Dy(1)-O(1)	76.4(2)	O(2)-Dy(1)-O(6)	147.95(11)	O(1)-Dy(1)-O(5)	148.76(13)	O(6)-Dy(1)-O(2)	116.36(18)
O(6)-Dy(1)-O(1)	75.9(2)	O(1)-Dy(1)-O(6)	139.51(10)	O(4)-Dy(1)-O(5)	121.26(14)	O(5)-Dy(1)-O(2)	75.9(2)
O(4)-Dy(1)-O(1)	121.0(2)	O(5)-Dy(1)-O(6)	73.39(10)	O(2)-Dy(1)-O(5)	77.09(12)	O(3)-Dy(1)-O(2)	140.60(19)
O(2)-Dy(1)-O(5)	78.3(2)	O(3)-Dy(1)-O(4)	72.91(11)	O(3)-Dy(1)-O(6)	114.90(13)	O(4)-Dy(1)-O(1)	148.51(16)
O(3)-Dy(1)-O(5)	143.6(2)	O(2)-Dy(1)-O(4)	80.43(11)	O(1)-Dy(1)-O(6)	138.71(13)	O(6)-Dy(1)-O(1)	81.64(16)
O(6)-Dy(1)-O(5)	72.8(2)	O(1)-Dy(1)-O(4)	118.62(11)	O(4)-Dy(1)-O(6)	76.23(13)	O(5)-Dy(1)-O(1)	122.98(18)
O(4)-Dy(1)-O(5)	77.8(2)	O(5)-Dy(1)-O(4)	75.78(11)	O(2)-Dy(1)-O(6)	141.50(12)	O(3)-Dy(1)-O(1)	75.53(16)
O(1)-Dy(1)-O(5)	138.4(2)	O(6)-Dy(1)-O(4)	84.32(10)	O(5)-Dy(1)-O(6)	72.10(12)	O(2)-Dy(1)-O(1)	71.47(17)
O(2)-Dy(1)-N(2)	144.4(2)	O(3)-Dy(1)-N(4)	141.70(12)	O(3)-Dy(1)-N(4)	148.87(14)	O(4)-Dy(1)-N(2)	70.21(18)
O(3)-Dy(1)-N(2)	81.2(2)	O(2)-Dy(1)-N(4)	79.86(11)	O(1)-Dy(1)-N(4)	71.30(14)	O(6)-Dy(1)-N(2)	145.79(19)
O(6)-Dy(1)-N(2)	104.8(2)	O(1)-Dy(1)-N(4)	81.58(12)	O(4)-Dy(1)-N(4)	79.43(14)	O(5)-Dy(1)-N(2)	77.24(19)
O(4)-Dy(1)-N(2)	78.7(2)	O(5)-Dy(1)-N(4)	71.83(12)	O(2)-Dy(1)-N(4)	115.78(14)	O(3)-Dy(1)-N(2)	118.70(18)
O(1)-Dy(1)-N(2)	142.8(2)	O(6)-Dy(1)-N(4)	97.85(11)	O(5)-Dy(1)-N(4)	131.20(13)	O(2)-Dy(1)-N(2)	70.40(19)
O(5)-Dy(1)-N(2)	72.7(3)	O(4)-Dy(1)-N(4)	145.32(12)	O(6)-Dy(1)-N(4)	71.52(13)	O(1)-Dy(1)-N(2)	129.51(18)
O(2)-Dy(1)-N(1)	150.7(2)	O(3)-Dy(1)-N(5)	79.57(11)	O(3)-Dy(1)-N(5)	147.69(14)	O(4)-Dy(1)-N(1)	98.33(18)
O(3)-Dy(1)-N(1)	74.7(2)	O(2)-Dy(1)-N(5)	131.75(11)	O(1)-Dy(1)-N(5)	103.91(14)	O(6)-Dy(1)-N(1)	150.25(17)
O(6)-Dy(1)-N(1)	73.4(2)	O(1)-Dy(1)-N(5)	71.96(11)	O(4)-Dy(1)-N(5)	137.54(14)	O(5)-Dy(1)-N(1)	136.64(17)
O(4)-Dy(1)-N(1)	132.4(2)	O(5)-Dy(1)-N(5)	117.55(11)	O(2)-Dy(1)-N(5)	76.94(14)	O(3)-Dy(1)-N(1)	76.43(17)
O(1)-Dy(1)-N(1)	82.5(2)	O(6)-Dy(1)-N(5)	71.69(11)	O(5)-Dy(1)-N(5)	76.58(13)	O(2)-Dy(1)-N(1)	75.54(18)
O(5)-Dy(1)-N(1)	113.1(2)	O(4)-Dy(1)-N(5)	146.15(11)	O(6)-Dy(1)-N(5)	73.94(14)	O(1)-Dy(1)-N(1)	76.65(17)
N(2)-Dy(1)-N(1)	62.9(2)	N(4)-Dy(1)-N(5)	63.87(11)	N(4)-Dy(1)-N(5)	62.86(14)	N(2)-Dy(1)-N(1)	62.73(19)

**Table S2.** Fitted parameters of the Cole-Cole plots for complex **1** at  $H_{dc} = 0$  Oe

T/K	$\chi_s$	$\chi_T$	$\tau$	$\alpha$
2.0	0.55985	5.50312	0.00065	0.16363
2.5	0.44278	4.44845	0.00066	0.16930
3.0	0.37911	3.73436	0.00066	0.17033
3.5	0.30114	3.22051	0.00066	0.18093
4.0	0.25098	2.83365	0.00065	0.18500
4.5	0.24585	2.52765	0.00064	0.18215
5.0	0.23575	2.28348	0.00063	0.17567
5.5	0.23354	2.08575	0.00061	0.16134
6.0	0.22469	1.90868	0.00057	0.14708
6.5	0.23110	1.76715	0.00053	0.13310
7.0	0.22878	1.64533	0.00047	0.11935
7.5	0.22156	1.53607	0.00041	0.10939
8.0	0.19548	1.44310	0.00036	0.10583
9.0	0.19983	1.28474	0.00027	0.09478
10.0	0.19615	1.15743	0.00019	0.09040
11.0	0.23509	1.05425	0.00014	0.09000
12.0	0.17717	1.27314	0.00014	0.10383

**Table S3.** Fitted parameters of the Cole-Cole plots for complex **2** at  $H_{dc} = 0$  Oe

T/K	$\chi_s$	$\chi_T$	$\tau$	$\alpha$
2.0	0.33535	5.39061	0.00088	0.16886
2.5	0.24490	4.32805	0.00087	0.17391
3.0	0.15060	3.62311	0.00085	0.18635
3.5	0.17581	3.11314	0.00087	0.17985
4.0	0.15246	2.73553	0.00087	0.18202
4.5	0.15357	2.43680	0.00086	0.17468
5.0	0.13182	2.20117	0.00086	0.17803
5.5	0.11451	2.00705	0.00083	0.17751
6.0	0.08163	1.84865	0.00080	0.18414
6.5	0.12232	1.71037	0.00080	0.16616
7.0	0.10653	1.58709	0.00076	0.15464
7.5	0.08916	1.48660	0.00071	0.15326
8.0	0.11142	1.38946	0.00067	0.12226
9.0	0.06160	1.24244	0.00054	0.13499
10.0	0.06431	1.11911	0.00043	0.11494
11.0	0.06000	1.01511	0.00033	0.09632
12.0	0.07550	0.93646	0.00026	0.09000

**Table S4.** Fitted parameters of the Cole-Cole plots for complex **3** at  $H_{dc} = 450$  Oe

T/K	$\chi_s$	$\chi_T$	$\tau$	$\alpha$
5.0	0.24900	2.34959	0.00767	0.20753
5.5	0.22869	2.11283	0.00483	0.16712
6.0	0.20829	1.92396	0.00318	0.13816
6.5	0.18841	1.77153	0.00216	0.11682
7.0	0.17350	1.64238	0.00152	0.09879
7.5	0.15857	1.53140	0.00110	0.08571
8.0	0.14901	1.43453	0.00081	0.07399
9.0	0.13599	1.27631	0.00048	0.05724
10.0	0.13542	1.15014	0.00030	0.04449

**Table S5.** Fitted parameters of the Cole-Cole plots for complex **4** at  $H_{dc} = 1500$  Oe

T/K	$\chi_s$	$\chi_T$	$\tau$	$\alpha$
2.0	0.08278	7.43298	0.01395	0.33352
2.5	0.08885	3.91051	0.26244	0.28004
3.0	0.07445	3.14714	0.10160	0.25658
3.5	0.06209	2.67374	0.04420	0.23510
4.0	0.04794	2.38222	0.02255	0.22759
4.5	0.02846	2.17562	0.01256	0.23349
5.0	0.01060	1.99724	0.00736	0.24148
5.5	0.02069	1.84965	0.00464	0.24959
6.0	0.03554	1.72154	0.00305	0.25077
6.5	0.05979	1.60490	0.00210	0.25531
7.0	0.09985	1.50478	0.00149	0.26058
7.5	0.01621	1.41017	0.00107	0.26466
8.0	0.02386	1.32655	0.00079	0.26758
9.0	0.03076	1.19391	0.00045	0.28482
10.0	0.03991	1.08172	0.00027	0.30423
11.0	0.06079	0.99127	0.00017	0.33097
12.0	0.08920	0.91112	0.00010	0.34822